Deuterium anions in inertial electrostatic confinement devices

D. R. Boris, E. Alderson, G. Becerra, D. C. Donovan, B. Egle, G. A. Emmert, L. Garrison, G. L. Kulcinski, J. F. Santarius, C. Schuff, and S. J. Zenobia

Fusion Technology Institute, University of Wisconsin–Madison, 1500 Engineering Drive, Madison, Wisconsin 53706, USA

A magnetic deflection-energy analyzer and Faraday trap diagnostic have been used to make measurements of divergent deuterium anion flow in the inertial electrostatic confinement experiment at the University of Wisconsin–Madison (UW-IEC) [J. F. Santarius, G. L. Kulcinski, R. P. Ashley, D. R. Boris, B. B. Cipiti, S. K. Murali, G. R. Piefer, R. F. Radel, I. E. Radel, and A. L. Wehmeyer, Fusion Sci. Technol. **47**, 1238 (2005)], a device to confine high-energy light ions in a spherically symmetric electrostatic potential well. Deuterium anion current densities as high as 8.5 $\mu A/cm^2$ have been measured at the wall of the UW-IEC device, 40 cm from the surface of the device cathode with a detector assembly of admittance area 0.7 cm^2. Energy spectra obtained using a magnetic deflection-energy analyzer diagnostic indicate the presence of D_2^-, and D^- ions produced through thermal electron attachment near the device cathode, as well as D^- ions produced via charge-transfer processes between the anode and cathode of the device.

I. INTRODUCTION

The inertial electrostatic confinement (IEC) fusion concept was first patented by Farnsworth [1] in the 1960s and was advanced by Hirsch shortly after Farnsworth's initial patent [2]. The concept focuses on confining light ions using large negative electrostatic potentials in a spherically symmetric geometry. Metallic electrodes are typically used to generate the potential well. Electrodes made of refractory metals are common due to their ability to withstand heavy heat loads from ion impact and sputtering.

By placing a smaller spherical cathode grid inside a grounded anode grid, ions produced outside the anode can be accelerated to fusion relevant energies (see Fig. 1). This confinement approach produces a non-Maxwellian plasma with increased ion density toward the center of the spherical geometry. The IEC device at the University of Wisconsin–Madison (UW-IEC) uses a 95% transparent cathode made of a tungsten-rhenium alloy. The IEC concept is of particular interest in the arena of nonelectric applications for fusion, such as neutron sources for clandestine materials detection, and possibly high-energy proton sources for medical isotope production [3,4]. This device is capable of operating in both a steady-state mode at up to 75 mA of total current, or operating in a pulsed mode exceeding 2 A of total current. All the measurments reported in this paper were performed with the UW-IEC device operating in a steady-state mode.

In typical gridded IEC devices, which operate at neutral gas pressures of 1–10 mTorr, atomic and molecular processes play a significant role since the mean free path for ions to interact with the background gas is on the order of the device size. Ions formed outside the anode, in a plasma source region, will undergo ionization, dissociative ionization, and charge-exchange processes as they are being accelerated by the electric field between the two grids. The contribution from atomic and molecular processes in IEC devices was first investigated by Black and Klevans [5]. Work on this topic was also performed by Thorson *et al.* [6] at the University of Wisconsin–Madison and, more recently, by Kh-

achan *et al.* at the University of Sidney [7]. An important phenomenon that has not been considered to date is the effect of reactions that create hydrogen or deuterium anions within IEC devices. In research reported here, these processes were considered and experimentally verified as important contributions to the ion flow within the UW-IEC device. The consideration of hydrogenic anions in IEC devices will considerably impact the physical models used describe IECs and devices like them. Indeed, it may aid in explaining the divergent particle flow measured recently in IEC-like hollow cathode devices [8,9].

Hydrogen anions are a much studied subject that holds important implications for ion sources involved in high-energy accelerators, ion-beam surface treatments, as well as neutral beam injection schemes for fusion plasmas [10,11]. The literature on negative-ion formation in hydrogen extends back to the 1950s when the first concepts for hydrogen anion sources were explored [12,13]

There are two processes of hydrogen anion formation that are particularly relevant for IEC devices, namely, electron
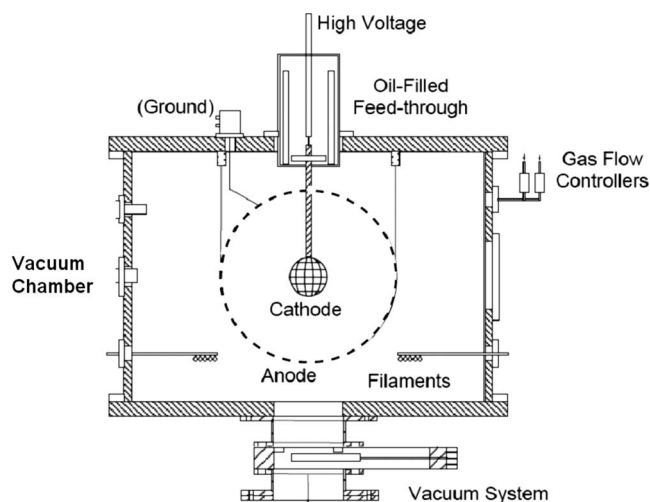
FIG. 1. Schematic of the University of Wisconsin IEC device.
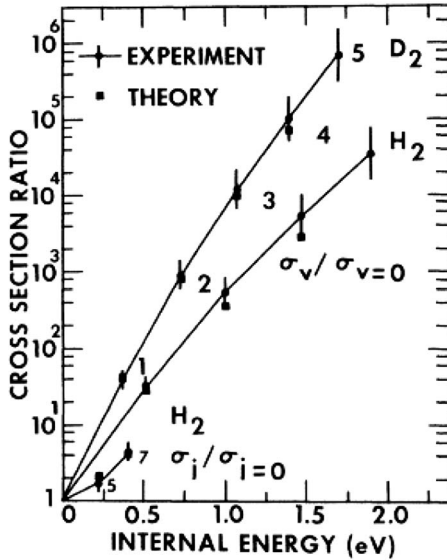
FIG. 2. The above data from Alan and Wong indicate cross section for dissociative thermal electron attachment in D_2 to vary between 8×10^{-24} cm^2 and $\sim 6 \times 10^{-18}$ cm^2 depending on the internal energy of the molecule [16].

attachment and charge transfer. Electron attachment, as the name implies, involves the attachment of a thermal electron to a neutral hydrogen gas molecule in an excited vibrational state [14], thus, producing a negatively charged hydrogen molecule. The formation of this H_2^- molecular ion is typically followed by its near instantaneous dissociation into H^- and an H atom. However, recent work has shown that metastable states of these hydrogenic molecular anions exist with lifetimes on the order of several to hundreds of μs.

Charge transfer in hydrogen occurs at much higher energies than electron attachment and involves a transfer of two electrons from background neutral gas to a positive ion moving through the neutral gas at high energy (~ 100 to $\sim 1 \times 10^4$ eV). This process was among the first means to produce negative ions by simply accelerating positive ions to the keV energy range and passing them through a gas target. In the following sections, the mechanics of charge transfer and electron attachment will be treated in more detail.

A. Dissociative thermal electron attachment to hydrogen

Thermal electron attachment to hydrogen molecules results in the dissociation of a hydrogen molecule into an H^- anion and neutral H atom. The time frame for this dissociation can range from a few fs to a few ms, depending on the rotational and vibrational states of the hydrogen molecule in question [15]. Amidst a population of thermal electrons ($kT \leq 1$ eV), the dissociative attachment reaction is such that hydrogen anions can become a significant fraction of the charge carriers in a low-temperature plasma (see Fig. 2). However, for long-lived metastable molecular anions to form, the molecule must be in highly excited angular momentum states. Modeling work done by Čížek *et al.* indicates that long-lived metastable states exist for $H_2^+ + H_2 \rightarrow H^- + 2H^+ + H$ when the angular momentum quantum number of

the molecular system J is greater than 25. Similar conditions exist for long-lived D_2^- formation [13], with J values in the range of 35–40. When these conditions are met metastable lifetimes exceeding hundreds of μs are possible,

$$D_2 + e \rightarrow D_2^{-(m)} \rightarrow D^- + D, \tag{1}$$
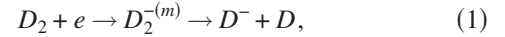
where the metastable lifetime $\tau = \sim 1 \ \mu s - \sim 1$ ms.

In IEC devices, the cathode region provides the necessary conditions for negative hydrogen ions to be produced through dissociative attachment. The neutral gas in glow discharge-type IEC devices is dispersed throughout the volume of the device so there is ample neutral gas located near the cathode. In addition, there is an abundant supply of thermal electrons produced from secondary emission at the cathode wires from positive-ion impact. Implanted deuterium in the cathode wires can also substantially contribute to D^- formation in the cathode region since vibrationally excited D_2 can be formed near the IEC cathode by recombinative desorption from the electrode surface followed by dissociative electron attachment of a slow electron [17]. Also, at high input power, cathode wires are typically heated to temperatures in the 1200 K range, which provide a means to excite the background hydrogen gas into the excited rotational states necessary for the formation of molecular hydrogen anions. While the worked cited above by Čížek *et al.* provides a mechanism for molecular anion formation, there was no available cross-section data for these processes at the time of this paper's publication. It may also be the case that sputtering of implanted hydrogen from the cathode wires could account for the production of excited hydrogen molecules that are susceptible to electron attachment. In either case, the J states of the hydrogen molecules produced near the cathode could be high enough to produce molecular hydrogen anions.

B. Charge transfer of hydrogen ions in IEC devices

As mentioned previously, charge transfer is fundamentally different from electron attachment in that it occurs between positive ions and background neutral gas at higher energies of a few keV. Positive hydrogen ions form three species, H^+, H_2^+, and H_3^+, all of which can undergo charge transfer to produce hydrogen anions when traversing a gas target. Examples are shown below,

$$H_3^+ + H_2 \rightarrow H^- + 2H^+ + 2H, \tag{2}$$

$$H_2^+ + H_2 \rightarrow H^- + 2H^+ + H, \tag{3}$$

$$H^{fast} + H_2 \rightarrow H^- + H^+ + H, \tag{4}$$

$$H^+ + H_2 \rightarrow H^- + 2H^+. \tag{5}$$
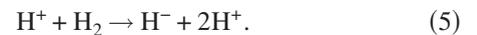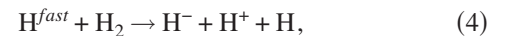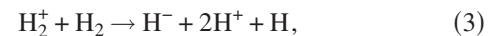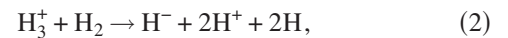
Observations of positive hydrogen and deuterium ion beams passing through gas targets of the same species indicate that a few percent of the beam current can be H^- or D^- ions upon exiting a gas target of sufficient thickness [18,19]. In IEC devices, positive ions will undergo continuous oscillations within the spherically symmetric potential well. This leads to an effective path length through the background neu-
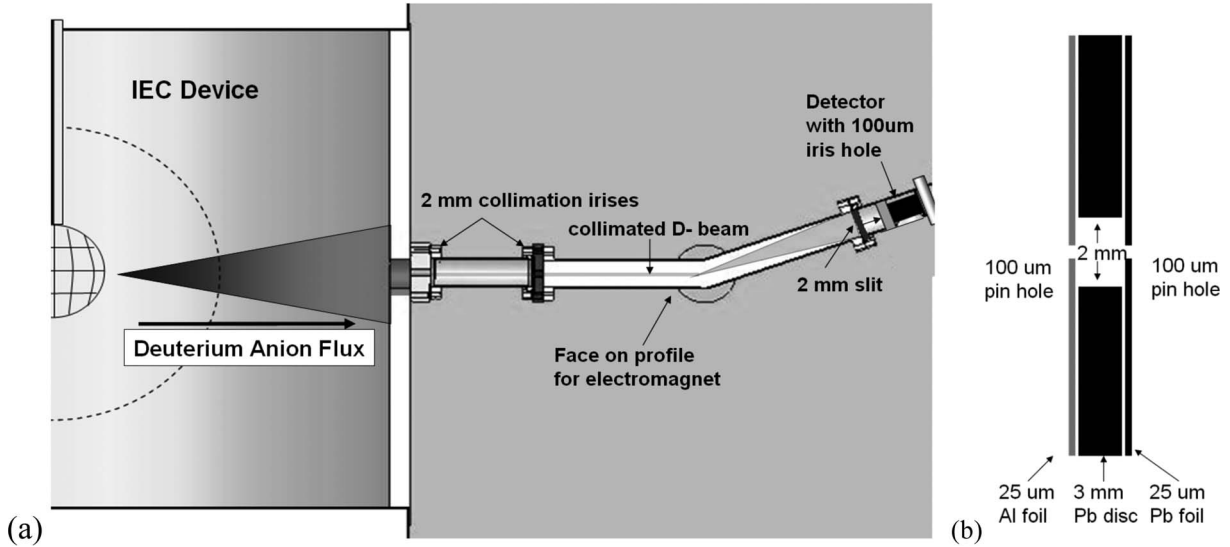
FIG. 3. (a) shows schematic of the magnetic deflection-energy analyzer. (b) shows a closeup of the construction of the 100 μm iris hole (not to scale) used to both limit particle flux to the detector and narrow the energy resolution of the diagnostic. The 100 μm iris sits on the face of the detector.

tral gas that can be much larger than the device dimensions. The positive ions in a gridded IEC device will eventually undergo one of four processes as they oscillate in the IEC potential well:

(1) The positive ion will be lost to a collision with the cathode grid.

(2) The positive ion will undergo nuclear fusion with either background gas or another ion.

(3) The positive ion will undergo a charge-transfer reaction that creates a fast neutral that is likely to leave the system, and a positive ion.

(4) The positive ion will undergo a charge-transfer reaction that creates a fast negative ion along with a cold positive ion.

The likelihood of producing negative ions through charge transfer is qualitatively significant provided that the grid transparency is sufficiently high to ensure that interactions with the background gas are more likely than interactions with the cathode.

II. DIAGNOSTICS DEUTERIUM ANION DETECTION IN IEC DEVICES

The detection of deuterium anions in the UW-IEC device was accomplished with two separate diagnostics:

(1) A magnetic deflection experiment, in which a variable electromagnet was used to measure the energy of negative ions with a specific charge to mass ratio streaming from the center of the UW-IEC device.

(2) A current collection plate with secondary electron suppression (Faraday trap) coupled with a weak permanent magnet tuned to deflect electrons emitted from the cathode but allow the detection of negative ions born within the anode of the UW-IEC device.

The magnetic deflection-energy analyzer was able to measure the energy spectra of negative ions in the UW-IEC de-

vice to a resolution of ± 1 keV. The Faraday trap was used as a means of confirming the presence of deuterium anions and to examine the manner in which the negative-ion current scales with the operation parameters of the UW-IEC device.

A. Magnetic deflection-energy analyzer

The magnetic deflection-energy analyzer diagnostic (Fig. 3) operates by first collimating the divergent flux of deuterium anions emanating from the IEC into a narrow beam with a pair of 2 mm diameter lead irises. This beam of deuterium anions is then passed through a variable electromagnet, which causes the beam to deflect in a direction perpendicular to both the velocity of the beam and the applied magnetic field. The angle of the deflection of an incoming particle, with charge q and mass m, when passing through a constant magnetic field $\vec{B}$ is given by the following expression:

$$\sin \theta_d = \frac{at}{v}, \tag{6}$$

where $a \equiv \left| \frac{q}{m} \vec{v} \times \vec{B} \right|$ is the magnitude of the acceleration due to the magnetic field, t is the time spent in the magnetic field, and v is the velocity of the ion. The time t can be defined as $t = l/v$, where l is the path length of the particle in the region of significant and nearly constant magnetic field. The acceleration due to the constant magnetic field can be expressed as

$$a = \frac{qpB}{m^2}, \tag{7}$$

where p and B are the magnitudes of the ion momentum and magnetic field, respectively. Thus, Eq. (6) can be re-expressed as

$$\sin \theta_d = \frac{qlB}{p}. \tag{8}$$

Equation (8) indicates that the deflection angle θ_d is dependent on the charge to mass ratio, the spatial extent of the magnetic field, and magnitude of the magnetic field.

Once the anions have been deflected by the electromagnet, they will continue toward the detector until they encounter a smaller lead iris with a diameter of 100 μm. This iris samples a narrow portion of the resulting fan-shaped beam of anions, consequently, isolating a narrow band of the velocity spectrum of deuterium anions emanating from the IEC device. A silicon-charged particle detector is used to detect the portion of the beam passing through the lead iris. Counts from the silicon charged particle detector are collected by a single-channel analyzer (SCA). The count rate in the SCA was recorded as a function of applied magnetic field from a GMW 5403 electromagnet with a 76-mm-diameter cylindrical cross-section magnet pole. The magnetic field was measured using a F.W. Bell 5070 Gauss meter with the transverse magnetic field probe mounted to the side of the bending section of the experiment. Spectra as a function of magnetic field were obtained using this setup. The SIMION [20] charged particle optics software package was then used to model and predict deuterium anion trajectories in the magnetic field produced by the GMW 5403 electromagnet. Thus, for the magnetic field settings applied during the experiments, the energy of anions directed into the charged particle detector could be calculated, yielding a measure of number of ions/(kev amu). The small iris allows the acquisition of high-resolution energy spectra of the deuterium anions. The resolution of the magnetic deflection-energy analyzer is dependent on the tenability of the electromagnet, the width of the final iris (100 μm in this case), and fidelity of the magnetic field simulations in SIMION. The magnetic field was measured to remain constant to within 50 G. Assuming an accurate simulation of the magnetic field structure energy resolution of ± 1 keV/nuclei is achievable using this setup. Energy spectra showing clear structure are shown in the following sections.

B. Experimental results: Magnetic deflection-energy analyzer

The energy analyzer diagnostic was used to examine the effects of cathode voltage and background pressure on the structure of the deuterium anion energy spectra. In all the spectra, there was structure indicating the presence of negative ions produced from the variety of processes mentioned previously, charge transfer, and thermal electron attachment. Figure 4 shows the voltage scan performed on the UW-IEC device with the cathode current and background pressure held constant at 30 mA and 2 mTorr, respectively. The spectra are shown offset from each other on the y axis to illustrate the manner, in which the spectra evolve as the cathode voltage is changed. The structure of the spectra can be fit by a four Gaussian structure. The three main Gaussian peaks can be accounted for by charge-transfer processes involving positive molecular deuterium ions moving at high energy in the intergrid region. The smaller peak at nearly the full cath-
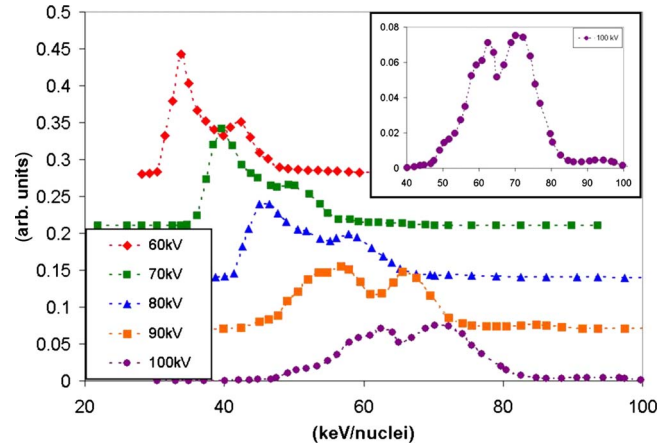
FIG. 4. (Color online) The deuterium anion spectra are plotted for several cathode voltages offset by 0.07 a.u. for every 10 kV. The cathode current and background pressure are held constant at 30 mA and 2 mTorr, respectively. The plots show a clear hardening of the spectra with increasing cathode voltage. In addition, the spectra change from being dominated by D_3^+/D^- at lower voltages (60–80 kV) charge-transfer ions to being dominated by D^+/D^- charge-transfer ions at higher voltages (90–100 kV). Error bars from counting statistics are negligible on the scale shown. Detail of 100 kV data set shown in upper right.

ode energy originates from thermal electron attachment to excited background gas near the hot cathode. An enhanced view of the 100 kV case is shown in the upper right-hand corner of Fig. 4.

A detailed view of the 100 kV case from Fig. 4 is shown in Fig. 5. Close observation of the 100 kV spectrum shows five peaks discernable in the data. The data were fit with a least-square fitting algorithm constrained to fit five Gaussians with positive amplitudes to the data set. In Fig. 5, these
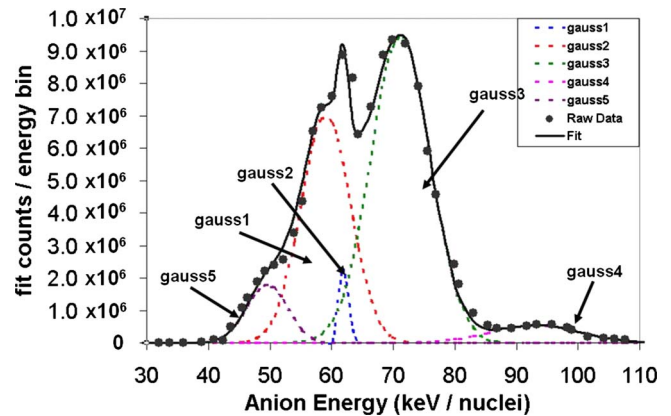
FIG. 5. (Color online) Detailed view of the 100 kV, 30 mA, and 2 mTorr data set. It shows the 5 Gaussian least-squares fit used to accurately replicate the structure from the data set. The fits "gauss1," "gausss2," and "gausss3" account for deuterium anions produced through D_3^+/D^-, D_2^+/D^-, and D^+/D^- charge-transfer reactions, respectively. The "gauss 4" fit is accounted for by D^- formed at the cathode via thermal electron attachment to background neutral gas. The "gauss5" fit is accounted for by metastable D_2^- formed via thermal electron attachment at the cathode.
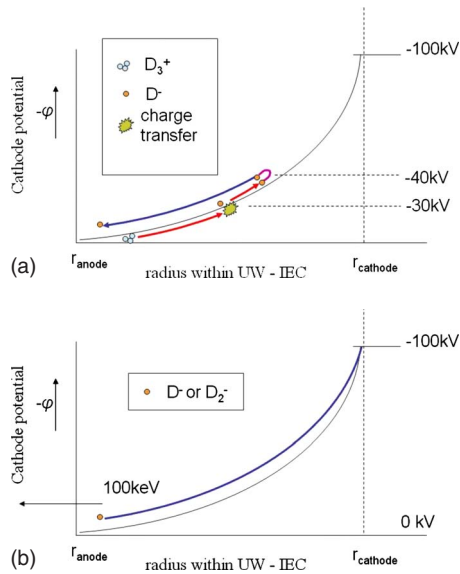
FIG. 6. (Color online) Illustrates examples of the resulting deuterium anion energies from (a) charge-transfer reactions in the intergrid region of the UW-IEC device and (b) thermal electron attachment near the cathode of the UW-IEC device. Note that the anions resulting from the thermal electron attachment will have 100 keV/anion so a D^- ion will have 100 keV and a D_2^- ion will have 50 keV/nuclei with the cathode at 100 kV.

peaks are denoted "gauss1," "gauss2," "gauss3," "gauss4," and "gauss5." The gauss1 through gauss3 peaks result from charge-transfer reactions, which occur in the intergrid region, where D_3^+ to D^-, D_2^+ to D^-, and D^+ to D^- reactions occur through the electron transfer process described earlier in this chapter. It should be noted that the narrowness of the gauss2 peak is somewhat artificial in this spectrum. The D_2^+ to D^- peak was not this narrow in the majority of other spectra taken with the magnetic deflection-energy analyzer. In addition, the 95% confidence intervals for the full width at half maximum of the gauss2 fit in this data set are quite large relative to the apparent width of the peak in the figure. The data set was chosen because it most prominently displays the gauss5 peak accounted for by D_2^- from thermal electron attachment near the cathode of UW-IEC device. The gauss4 peak results from D^- formed via dissociative thermal electron capture, also near the cathode of the UW-IEC device. The anions in gauss4 and gauss5 are detected with the full cathode energy.

A schematic of the charge-transfer process is shown in Fig. 6(a). In this figure, the initial incoming D_3^+ ion undergoes a charge transfer after it has acquired 30 keV of kinetic energy from the potential well. Upon undergoing charge transfer, the resulting D^- anion still has 10 keV of radially inward directed kinetic energy. This is because the kinetic energy of the initial D_3^+ ion is divided between three nuclei. Thus, the D^- anion continues to a position in the potential well with -40 kV of potential. The D^- anion is then accelerated out of the device with 40 keV of kinetic energy, which can be detected in the magnetic deflection-energy analyzer. Figure 6(b) illustrates the process of thermal electron attachment that can occur with excited gas molecules near the cathode.
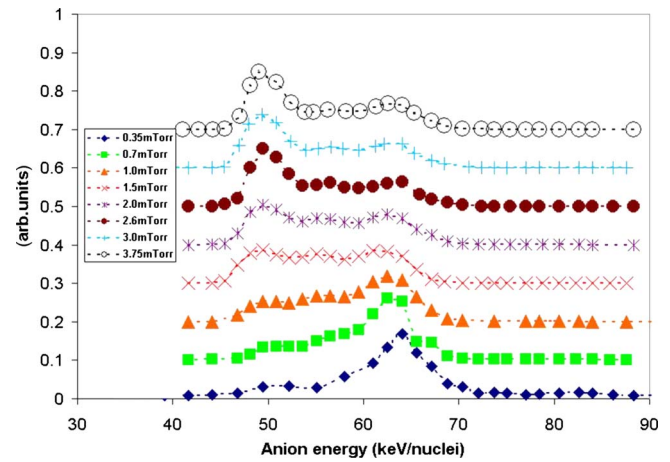
FIG. 7. (Color online) Pressure scan with cathode voltage and cathode current held constant at 90 kV, and 30 mA, respectively. Note that the ratio of the D_3^+/D^- peak to the D^+/D^- peak changes dramatically over the scan. Each successive data set is offset by 0.1 a.u.

With the formation occurring in the region of relatively flat potential within the cathode, the anions are able to attain full energy as they are accelerated out of the system by the anode-cathode potential difference. However, the magnetic deflection-energy analyzer measures the kinetic energy/amu of the anions. Thus, a full cathode energy D_2^- ion will be measured at the same deflection angle as a D^- ion with half the cathode energy.

A scan of the background neutral gas pressure was also performed on the UW-IEC device with results shown in Fig. 7. The pressure scan was performed with the cathode voltage and cathode current held constant at 90 kV and 30 mA, respectively. The charge-transfer peaks are most prominent in this data set, and the data indicate that the charge-transfer peaks are significantly affected by changes in the neutral gas pressure. At low pressures (0.35–1 mTorr), the D^+ to D^- peak dominates the spectra. At high pressures (2–3.75 mTorr), the D_3^+ to D^- peak dominates the spectra. Between these two pressure regimes is a transition region. This is most likely linked to changes in the molecular ion species mix in the source region plasma and intergrid region as the pressure is varied [21].

C. Discussion: Magnetic deflection-energy analyzer results

The energy spectra obtained by the magnetic deflection-energy analyzer indicate that the anion creation processes of charge transfer and thermal electron attachment are significant to the operation of IEC devices, in which a substantial background neutral pressure (>0.1 m Torr) is present. Pictorial representations of the two processes are shown in Fig. 7. Of particular interest is the significant contribution from what appear to be D_2^- ions in Fig. 5. This work corroborates experimental results by Ober *et al.* [22] and Golser *et al.* [23] that measured long-lived metastable molecular anion states for deuterium and hydrogen. The mean lifetime of these metastable states varied from ~ 1 μs to ~ 1000 μs. The distance of the anion detector from the cathode indicates that

the detected D_2^- had a minimum lifetime of ~0.5 μs. This is consistent with the experimental and theoretical results mentioned previously.

This previous work provides a reasonable explanation for the signature of D_2^- ions in the energy spectra measured by the magnetic deflection-energy analyzer. The cathode of the UW device reaches temperatures in the range of 1200 K. In this temperature regime, the production of metastable molecular deuterium anions is possible, since the neutral gas near the cathode wires would likely be in excited rotational and vibrational states. In the presence of these excited neutral gas molecules is an abundance of thermal electrons created by secondary and thermionic electron emission from the cathode wires. Qualitatively, this implicates the cathode region of the UW-IEC device as an ideal place for molecular deuterium anions to form. If D_2^- ions are formed near the cathode, the lifetimes of these metastable states are sufficient to allow the molecular anions to be accelerated out of the device and into the energy analyzer's charged particle detector before the molecular ion dissociates. Thus, it is reasonable to expect the presence of the molecular deuterium anions within a gridded IEC device. An unexpected result from this work is the D_2^-/D^- ratio for those anions resulting from electron attachment near the cathode. Previous measurements of this ratio were made on experiments using cesium sputtering to create molecular anions. The D_2^-/D^- ratios were $\sim10^{-5}$ as reported by Golser *et al.* [23]. The D_2^-/D^- ratio measured in the UW-IEC device were 0.5–1; many orders of magnitude higher.

Measurement of D_2^-/D^- ratios on this scale is not unprecedented. Similar findings indicating D_2^-/D^- ratios of ~0.35–0.4 were reported by Wang *et al.* [24] in 2007. These measurements were performed on dielectric barrier discharge plasmas in hydrogen and deuterium. The electrode voltages for these experiments were ~10–15 kV.

D. Faraday trap diagnostic

The Faraday trap diagnostic operated by collecting negative ions on a 0.7-cm^2-aluminum current collection plate and suppressing the emission of secondary electrons from the plate with a transparent steel mesh biased to -50 V relative to the collection plate. With the UW-IEC device in operation, this configuration resulted in a negative current corresponding to the collection of electrons and negative ions diverging from the center of the UW-IEC device.

A current collection diagnostic such as this must somehow isolate the charged particle signal from negative ions streaming out from the IEC, from the signal from secondary electrons born by fast positive-ion impact at the device cathode. These secondary electrons born at the cathode will stream out from the device, with high kinetic energy, just as do deuterium anions. In order to isolate the negative ions from the high-energy electrons, a set of weak permanent magnets were used to create a ~100 G magnetic field transverse to the electron trajectory. This served to deflect the high-energy electrons away from the collection plate, while leaving the trajectory of the negative ions relatively unperturbed. This is illustrated in Fig. 8.
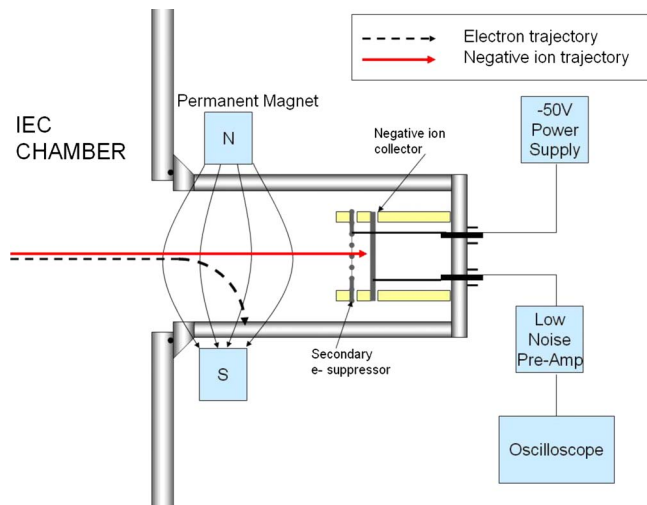
FIG. 8. (Color online) Shows a schematic of the Faraday trap diagnostic illustrating differing negative-ion and electron trajectories. The negative-ion collector plate and secondary electron suppressor grid are isolated from the chamber and each other by ceramic standoffs. The magnetic field is 100 G, and its orientation has been rotated by 90° in the image above so as to show the spatial extent of the magnetic field.

The secondary electron suppressor grid is isolated from the negative-ion collector plate by ceramic standoffs, and both of these metallic components are isolated from the chamber by additional standoffs. The negative-ion current collected by the Faraday trap is fed to a Stanford Research Systems SR-570 low noise current preamplifier through isolated BNC feedthroughs. The preamplifier provides +5 V of bias to drive the negative-ion signal collection. The amplifier is able to measure negative-ion currents a fraction of a nanoamp reliably on the 1 nA/V amplification setting. This signal is then fed to a Tektronix TDS-220 oscilloscope. This allowed the total negative-ion current to be measured in addition to the spectral measurements made with the magnetic deflection-energy analyzer diagnostic. The Faraday trap diagnostic took measurements at two locations on the UW-IEC device. These are shown below in Fig. 9.

The two locations collected vastly different amounts of the negative-ion current emanating from the UW-IEC device. Position 1's view of the device was moderately obstructed by a cross in the anode wires, whereas position 2 was aligned for its view to be roughly centered through anode and cathode channels. The resulting data obtained from these two positions will be detailed in the following section [25].

E. Experimental results: Faraday trap

The Faraday trap diagnostic was able to show that negative ions were being collected by showing that negatively charged particles were still impacting the collector plate even in the presence of a 100 G magnetic field. The UW-IEC device is capable of generating electrons with a maximum energy of 200 keV. It is not possible for electrons of this energy to both traverse the 100 G magnetic field and maintain a trajectory that intersects the Faraday trap collector.
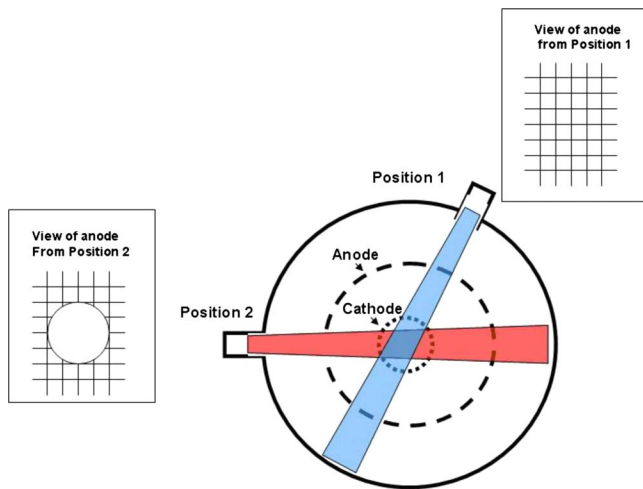
FIG. 9. (Color online) Shows the two positions and corresponding lines of site on which the Faraday trap diagnostic was oriented.

FIG. 10. (Color online) The schematic above shows a two-dimensional (2D) cylindrical representation of the potential profiles between an IEC cathode and anode with -100 kV on the cathode. The perturbations near the cathode in the 2D representation are $\sim 5 - 10$ kV. This will be reduced in a 3D geometry but still substantial for cold anions and electrons born near the cathode.

Measurement of the fraction of the current into the Faraday trap due to deuterium anions and electrons, respectively, was performed by measuring the collector current with and without the deflection field in place. The deflection field was then increased to 400 G to show that the negative ions were not substantially perturbed by the presence of the deflection field. The 0–100 G change results in an 18% decrease to collector current, effectively accounting for the fraction of the current resulting from secondary electrons from the cathode. Further increasing the magnetic field from 100 to 400 G results in a 2% decrease in collector current, illustrating that the remaining negative ions should be essentially unperturbed by the initial 100 G field used to deflect the secondary electrons. This data also give the surprising result that, at least along the field of view of the Faraday trap (position 2 in this case), secondary electrons make up a relatively minor portion (18%) of the diverging current in the device. This may be an effect of channels of electron and anion current caused by the cathode geometry. Potential perturbations brought about by the discrete nature of the cathode grid wires in an IEC device likely play a major role in determining the flow of charged particles, particularly, negative charged particles. Figure 10 shows a schematic of potential perturbations around the grid wires of a cylindrical IEC cathode, and the spherical cathode of the present study will have analogous three-dimensional (3D) perturbations.

The variations in potential near the grid wires can act as a mechanism to focus anions and electrons born near them in the relatively field free region within the cathode. Such focusing would result in channels of negative charged particle flow. The spatial extent of such channels would be on the order of the holes formed by the cathode wires. The beams should have a focal length dependent on the mass of the charged particles being focused, the cathode voltage, and the cathode geometry. Well-focused beams of anions and electrons could lead to regions of negative space charge that affect the positive-ion flow within the device. The mapping of these ion flow channels will be the subject of future work.

The Faraday trap was used to parametrize the deuterium anion current when varying cathode voltage and neutral gas

pressure in the UW-IEC device. These characteristics were examined at Faraday trap positions 1 and 2 to get a qualitative picture of the uniformity of the anion current. The deuterium anion current and the electron current were found to be highly nonuniform between positions 1 and 2. At position 1, no electron current was measured compared to ~ 0.75 μA at position 2. Similarly, the deuterium anion current measured at position 2 was a factor of 5 higher than at position 1. Qualitatively, this suggests the presence of a channel of negative ion and electron current at position 2. At position 2, the collector current varied between 2 and 6 μA nominally. A crude estimate on the total deuterium anion current in the system can be calculated by assuming the collector plate was perfectly aligned with the suspected anion microchannel and that all the current in the microchannel was collected by the Faraday trap. Since the UW-IEC cathode used in this experiment has 230 such channels in total, a rough estimate of the total anion current is approximately 0.5–1.5 mA.

Parametrics of the deuterium anion current were performed for varying cathode voltage, cathode current, and neutral gas pressure. Thus, for this particular line of sight through the chamber scaling laws for varying conditions could be obtained. In all of the parametric studies, it should be noted that the collected current represents the flux of anions that actually gets through the background neutral gas to the detector. The anion flux may vary significantly with radius, and this would not be discernable from the Faraday trap diagnostic in its current configuration.

1. Pressure scan

A pressure scan of the deuterium anion current was performed with the cathode at 100 kV. The cathode current was held constant at 30 mA over the course of the experiment and the neutral gas pressure was varied between 0.5 and 4 mTorr. This represents the standard operation regime
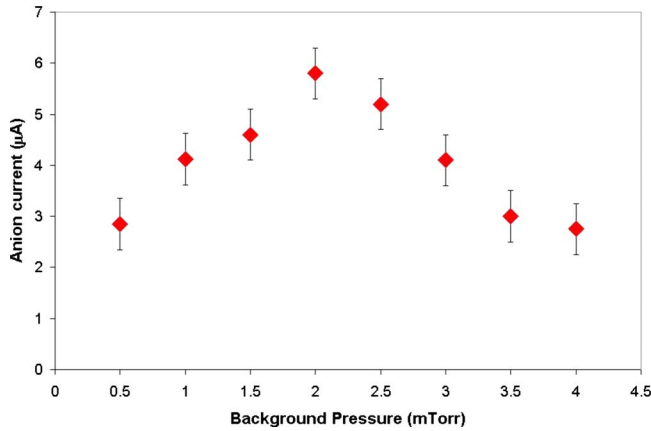
FIG. 11. (Color online) This pressure scan (−100 kV of cathode voltage and 30 mA of cathode current) illustrates how the deuterium anion current detected in the Faraday trap has a maximum for 2 mTorr of background gas. This is due to increasing neutral pressure resulting increasing anion creation up to 2 mTorr with further increases in background pressure resulting in attenuation of the anion flux to the detector.

of the UW-IEC device. The data for the pressure scan are shown in Fig. 11.

The anion flux to the collector peaks at 2 mTorr followed by decreasing detected current at higher pressures. The likely interpretation of this peak is that from 0.5 to 2 mTorr, the increased pressure serves as a source for anion creation, leading to greater anion flux detected at the collector of the Faraday trap. At pressures greater than 2 mTorr, the increased gas pressure begins to attenuate the anion flux incident on the collector plate. Thus, the measured current decreases. This experiment was repeated at positions 1 and 2 with similar scaling found at both positions.

2. Voltage scan

The voltage scan performed using the Faraday trap showed significant variability between the two positions. In position 1, the collector received between 0.5–1.5 μA of current with a peak current between 40 and 50 kV on the cathode. Moving the collector to position 2 resulted in roughly a factor of 5 increase in collected current and a dramatically different profile to the collector current and voltage curve (see Fig. 12). What is clear from this data is that the deuterium anion flux is highly dependent on the chamber geometry with the dominant factor, most likely, being the cathode wire orientation. Potential variations due to nonuniformities in the cathode (namely grid wires) can result in perturbations that will focus the negative ions, and secondary electrons, into channels. It is likely that position 1 is outside one of these channels and that position 2 is better aligned with one of the potential channels generated by the cathode.

The rollover of anion current with voltage may be related to two separate factors. First, as voltage is increased the positive ions undergoing charge transfer are accelerated to energies past the peak of the charge-transfer cross section (∼60 keV for D_3^+ ions). A second possibility is that the focusing effect of the grid wires optimally focuses the deute-
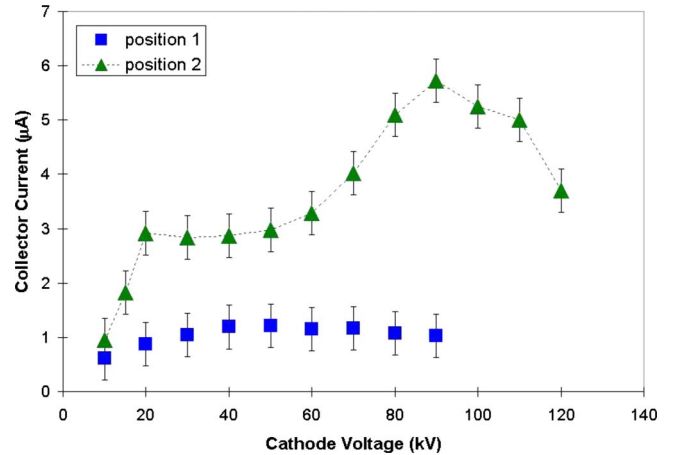
FIG. 12. (Color online) Position 1 shows a sublinear dependence of collector current on voltage, with a maximum between 40 and 50 kV. Position 2 shows a greater than linear dependence of collector current on voltage with a maximum at 90 kV. At both positions, the cathode current was 30 mA and the background pressure was 2 mTorr.

rium anion flux onto the collector plate at near 90 kV on the cathode. Above and below this value, the negative-ion flux is either under focused or over focused, resulting in a lower current measured by the Faraday trap. It may be that both of these effects are contributing to the scaling observed in the voltage scan.

These assertions require further experiments to more definitively map the deuterium anion current in the UW-IEC device. A detailed mapping of the beam channels with a multichannel array of Faraday cups would answer many of the questions regarding the geometry of the anion and electron flux. Such an experiment would also quantitatively assess the contributions of the anions and electrons to total cathode current in the UW-IEC device.

III. CONCLUSIONS

Using a magnetic deflection-energy analyzer, deuterium anions resultant from both charge-transfer and thermal electron attachment processes have been measured in the UW-IEC device. In addition, long-lived molecular deuterium anions have been measured with metastable lifetimes of at least 0.5 μs. These molecular anions were detected with the full cathode energy, indicating that they originated near the hot cathode at the center of the IEC device.

A Faraday trap diagnostic was used to corroborate the data from the magnetic deflection-energy analyzer and to make measurements of deuterium anion current at two positions around the UW-IEC device. This diagnostic indicated that the deuterium anion current was highly variable with angular position, indicating a strong dependence on device geometry. In addition, a total anion current of ∼1 mA was calculated from the Faraday trap measurements. Further work is recommended to more definitively map the angular dependence of deuterium anion intensity and to determine the extent to which IEC devices can produce molecular hydrogenic anions.

[1] P. T. Farnsworth, U.S. Patent No. 3,258,402 (June 28, 1966).

[2] R. L. Hirsch, J. Appl. Phys. **38**, 4522 (1967).

[3] G. L. Kulcinski, J. W. Weidner, B. B. Cipiti, R. P. Ashley, J. F. Santarius, S. K. Murali, G. R. Piefer, and R. F. Radel, Fusion Sci. Technol. **44**, 559 (2003).

[4] G. L. Kulcinski and J. F. Santarius, J. Fusion Energy **17**, 17 (1998).

[5] W. M. Black and E. H. Klevans, J. Appl. Phys. **45**, 2502 (1974).

[6] T. A. Thorson, R. D. Durst, R. J. Fonck, and A. C. Sontag, Nucl. Fusion **38**, 495 (1998).

[7] J. Khachan, D. Moore, and S. Bosi, Phys. Plasmas **10**, 596 (2003).

[8] J. Kipritidis, J. Khachan, M. Fitzgerald, and O. Shrier, Phys. Rev. E **77**, 066405 (2008).

[9] J. Kipritidis and J. Khachan, Phys. Rev. E **79**, 026403 (2009).

[10] G. Ian, in *The Physics and Technology of Ion Sources*, edited by I. G. Brown (Wiley, New York, 2004).

[11] J. Peters, Rev. Sci. Instrum. **71**, 1069 (2000).

[12] B. Stier, Phys. Rev. **103**, 896 (1956).

[13] T. Phillips, Rev. Sci. Instrum. **27**, 97 (1956).

[14] R. K. Janev, W. D. Longer, K. Evants, Jr., and D. E. Post, Jr., *Elementary Processes in Hydrogen-Helium Plasmas* (Springer-Verlag, Berlin, 1987).

[15] M. Čížek, J. Horáček, and W. Domcke, Phys. Rev. A **75**, 012507 (2007).

[16] M. Allen and S. F. Wong, Phys. Rev. Lett. **41**, 1791 (1978).

[17] M. Bacal, Rev. Sci. Instrum. **79**, 02A516 (2008).

[18] S. K. Allison, Rev. Mod. Phys. **30**, 1137 (1958).

[19] S. F. Philp, J. Appl. Phys. **31**, 1592 (1960).

[20] Computer code SIMION® Version 8 (Scientific Instrument Services, Inc).

[21] D. R. Boris and G. A. Emmert, Phys. Plasmas **15**, 083502 (2008).

[22] O. Heber, R. Golser, H. Gnaser, D. Berkovits, Y. Toker, M. Eritt, M. L. Rappaport, and D. Zajfman, Phys. Rev. A **73**, 060501 (2006).

[23] R. Golser, H. Gnaser, W. Kutschera, A. Priller, P. Steier, A. Wallner, M. Čížek, J. Horáček, and W. Domcke, Phys. Rev. Lett. **94**, 223003 (2005).

[24] W. Wang, Y. Xu, A. Zhu, Z. Liu, X. Liu, and X. Yang, J. Phys. B **40**, 921 (2007).

[25] J. F. Santarius, G. L. Kulcinski, R. P. Ashley, D. R. Boris, B. B. Cipiti, S. K. Murali, G. R. Piefer, R. F. Radel, I. E. Radel, and A. L. Wehmeyer, Fusion Sci. Technol. **47**, 1238 (2005).